Hindawi Publishing Corporation
Journal of Nanomaterials
Volume 2010, Article ID 948941, 7 pages
doi:10.1155/2010/948941

Research Article

Synthesis of Silver Nanoparticles by Precipitation in Bicontinuous Microemulsions

Pamela Y. Reyes, Jesús A. Espinoza, María E. Treviño, Hened Saade, and Raúl G. López

Centro de Investigación en Química Aplicada, Boul. Ing. Enrique Reyna No. 140, Saltillo, Coahuila 25253, Mexico

Correspondence should be addressed to Raúl G. López, glopez@ciqa.mx

Received 21 December 2009; Accepted 9 March 2010

Academic Editor: Sherine Obare

Silver nanoparticles precipitation was carried out at 70°C in bicontinuous microemulsions stabilized with a mixture of surfactants sodium bis (2-ethylhexyl) sulfosuccinate/sodium dodecyl sulfate (2/1, w/w) containing an aqueous solution of 0.5 M silver nitrate and toluene as organic phase. Various concentrations of aqueous solution of sodium borohydride (precipitating agent) and their dosing times on microemulsions were studied. Regardless of dosing time, higher and medium concentrations of precipitating agent promoted the formation of worm-like nanostructures, while the lowest concentration allowed to obtain a mixture of isolated silver nanoparticles (mean diameter ≈ 3 nm) and worm-like nanostructures. Experimental yields much higher than those typical in precipitation of silver nanoparticles in reverse microemulsions were obtained. An explanation for formation of worm-like nanostructures based on the development of local zones inside the microemulsions channels with high particle concentrations was proposed.

1. Introduction

Nowadays, silver nanoparticles attract significant attention for biomedical applications due to their great biocompatibility and biocide properties [1–6]. A critical feature for the development of such applications is the size of nanoparticles. The biocide power of silver nanoparticles depends on their ability for ions release, which is directly related to their overall superficial area. Because of the increase in the area/volume ratio as nanoparticle size decreases, nanoparticle dimensions as small as possible are desirable, in order to increase efficiency. Precipitation in reverse microemulsions [7–16] is a method that allows obtaining particles with diameters smaller than 10 nm and narrow particle size distributions. Nevertheless, the main drawback of this method is its low yield. Although none of the reports on silver nanoparticles precipitation in reverse microemulsions found in our literature search shows experimental yields, calculations based on available data in these reports reveal that theoretical yields range from near 0.1 [7–9, 11, 13] to 0.4 g [10] silver nanoparticles per 100 g reaction mixture. This feature of the method is due to the low concentration of the aqueous phase (normally ≤15 wt.%) that reverse microemulsions usually can contain. Unlike reverse microemulsions, bicontinuous microemulsions can have up to 40–50 wt.% concentration of the aqueous phase [17]. This is due to differences in nanostructure; while reverse microemulsions are made up of nanodroplets of the aqueous phase dispersed in an oleic continuous phase, bicontinuous microemulsions are formed by interconnected aqueous channels with diameters usually less than 10 nm, immersed in an oleic continuous phase [17]. Because of the higher aqueous phase concentration (where precipitation reactions occur), it is expected that an increase in the yield of precipitated silver nanoparticles could be achieved through the use of bicontinuous microemulsions. As far as we know, there are no reports about the preparation of silver nanoparticles by precipitation in this type of microemulsions. Nevertheless, recently we demonstrated that precipitation in bicontinuous microemulsions is a method that allows to produce magnetic nanoparticles with an average particle diameter less than 10 nm and narrow particle size distribution [18, 19].

Table 1: Amount and concentration of $NaBH_4$ aqueous solution and their dosing time in the precipitation reactions in bicontinuous microemulsions.

Run	$NABH_4$ solution		Dosing time (min)
	(M)	(g)	
LC1	1.250	15.0	100
LC2	1.250	15.0	110
MC1	1.875	10.0	100
MC2	1.875	10.0	110
HC1	2.840	6.6	100
HC2	2.840	6.6	110

We report here the use of bicontinuous microemulsions as media for obtaining silver nanoparticles. The precipitation reactions took place at 70°C by adding an aqueous solution of sodium borohydride ($NaBH_4$) to microemulsions containing an aqueous solution of silver nitrate ($AgNO_3$) stabilized with the mixture of surfactants sodium bis (2-ethylhexyl) sulfosuccinate (AOT)/sodium dodecylsulfate (SDS), in a weight ratio of 2/1, and toluene like organic phase. The effect of dosing time and concentration of $NaBH_4$ aqueous solution on morphology and particle size was studied.

2. Materials and Methods

2.1. Materials. $AgNO_3$ (>99%), $NaBH_4$ (>98%), SDS (>98.5%), and toluene (>99.8%) from Aldrich and AOT (>96%) from Fluka were used as received. Water was of tridistilled deionized grade.

2.2. Synthesis of Silver Particles. Precipitation reactions were carried out at 70°C in a 100 mL jacketed glass reactor equipped with a reflux condenser and an inlet for $NaBH_4$ aqueous solution feed. Composition of the bicontinuous microemulsions was the same in all precipitation reactions, and it was chosen based on electrical conductivity measurements of selected samples of mixtures AOT/SDS (2/1, wt./wt.), 0.5 M $AgNO_3$ aqueous solution, and toluene. The chosen microemulsion was composed of 35 wt.% surfactant, 30 wt.% 0.5 M $AgNO_3$ aqueous solution, and 35 wt.% toluene. The typical procedure for the precipitation reaction started with loading the reactor with the microemulsion (100 g) and then raising temperature to 70°C. After that, the required amount of aqueous solution of $NaBH_4$ was dosed drop by drop in a predetermined time to the reactor. In order to preserve the nanostructure in bicontinuous microemulsions, agitation was not provided during the reactions. In all reactions, the molar ratio $NaBH_4/AgNO_3$ was equal to 1.25, that is, 25% higher than the stoichiometric ratio. Table 1 shows the different amounts and concentrations of aqueous solution of $NaBH_4$ dosed at 100 and 110 min. After addition, completion reaction was allowed to proceed for 30 min and then acetone was added to precipitate the solids in the final reaction mixture. Afterwards, the precipitate was washed at least seven times with water-acetone (81/19, wt./wt.) and then dried. Three samples from the final product were taken for analyzing by X-ray diffraction, Atomic Absorption Spectroscopy and Transmission Electron Microscopy (TEM).

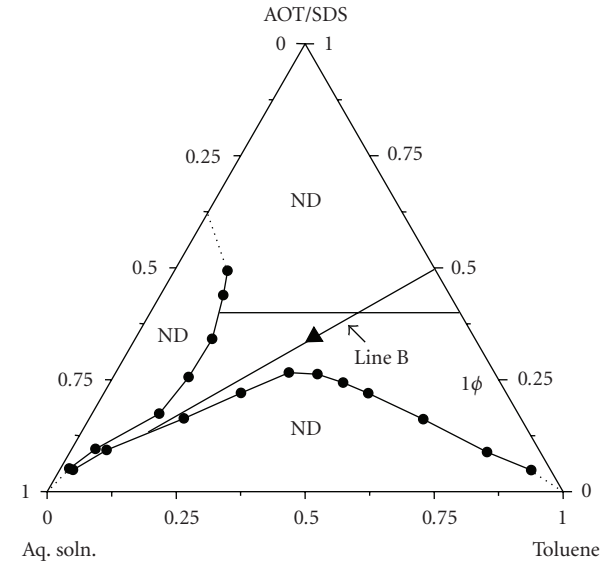

Figure 1: Composition of the bicontinuous microemulsion where precipitation reactions were carried out (▲). Line B indicates the constant surfactant/toluene weight ratio at which electrical conductivities were measured. Diagram phase was reproduced from [20].

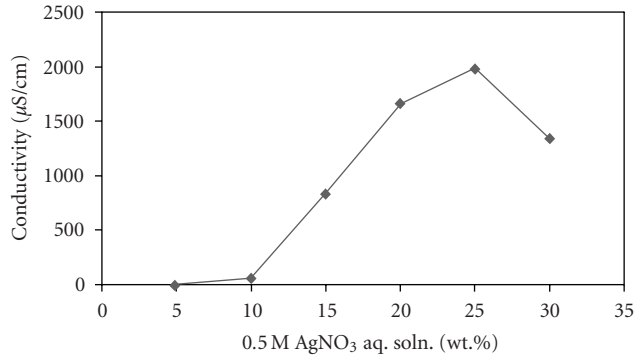

Figure 2: Electrical conductivities at 70°C of microemulsions at different concentrations of 0.5 M $AgNO_3$ aqueous solution along the composition line B of Figure 1.

2.3. Characterization. Electrical conductivities were measured at 70°C and 1 KHz with a Hach sension 5 conductivity meter. X-ray analyses were performed with a Siemens D-5000 X-ray Diffractometer. The silver content in the final powder was determined by Atomic Absorption Spectroscopy in a Varian Spectra 250 AA equipment. Particle size was determined by TEM in a Titan-300 kV, for which, samples were prepared by dispersing the resulting powders in acetone with ultrasonication and then depositing the dispersion on a copper grid.

3. Results and Discussion

The phase diagram of the system AOT/SDS (2/1, wt./wt.), 0.5 M $AgNO_3$ aqueous solution, and toluene at 70°C was previously reported by our group [20]. This diagram shows a wide transparent region (1ϕ), which corresponds to a microemulsion region. Here, in Figure 1 we reproduce the phase diagram modified by inclusion of a line (B), which represents a 50/50 weight ratio of surfactant/toluene. The results of electrical conductivities measured along line B are shown in Figure 2. It can be seen here that samples with aqueous solution contents lower than 10 wt.% show conductivity values <60 μS/cm. According to literature very low electrical conductivities are characteristics of reverse microemulsions, because the discontinuity in their nanostructure [21, 22]. Based on this and the transparency and fluidity of those samples, it is believed that they are reverse microemulsions. A further increase in aqueous solution content leads to an abrupt increase in conductivity between 10 and 15 wt.%, to reach around 2,000 μS/cm at 25 wt.% aqueous solution. Then, at 30 wt.%, conductivity diminishes to around 1,350 μS/cm. The great increase in conductivity values with aqueous solution content suggests a transition from reverse to bicontinuous microemulsions, because the higher conducting capacity of the latter arising from their continuous aqueous phase [22–26]. In fact, determination of transition from reverse to bicontinuous microemulsions based on the change of electrical conductivity as a function of aqueous phase content is a well-documented practice [26–30]. So, it is concluded that bicontinuous microemulsions are formed along line B ranging from some point between 10 and 15 wt.% to at least 30 wt.% aqueous solution.

To study the precipitation of silver nanoparticles in bicontinuous microemulsions at high aqueous phase content, a microemulsion composed of 30 wt.% 0.5 M $AgNO_3$ aqueous solution, 35 wt.% surfactant, and 35% wt. toluene was chosen. The triangle in Figure 1 indicates the composition of the selected microemulsion.

The appearance of precursor microemulsions in all runs was yellowish-translucent but it turned to black upon the starting addition of $NaBH_4$ aqueous solution. After the end of reactions the precipitate was washed and recovered as a grayish-black powder. Figure 3 shows the X-ray diffraction pattern of purified product samples from runs LC1and LC2 and the standard patterns of silver and $AgNO_3$. The samples patterns show the characteristic signals for the diffraction pattern of silver crystals, while there are no signals for $AgNO_3$ crystals or for other possible silver compounds, for example, AgO, which could have formed during the washing process. X-ray diffraction patterns of samples from the rest of runs (not shown) also reveal that all the silver that they contain is as silver crystals.

TEM micrographs of samples from runs HC1, HC2, MC1, and MC2 are shown in Figure 4. From these micrographs it is evident that silver precipitated in nanostructures and sizes different to those characteristics of silver synthesized in reverse microemulsions [7–16]. In an inspection of all micrographs obtained of samples from runs HC1, HC2, MC1, and MC2, mainly worm-like nanostructures

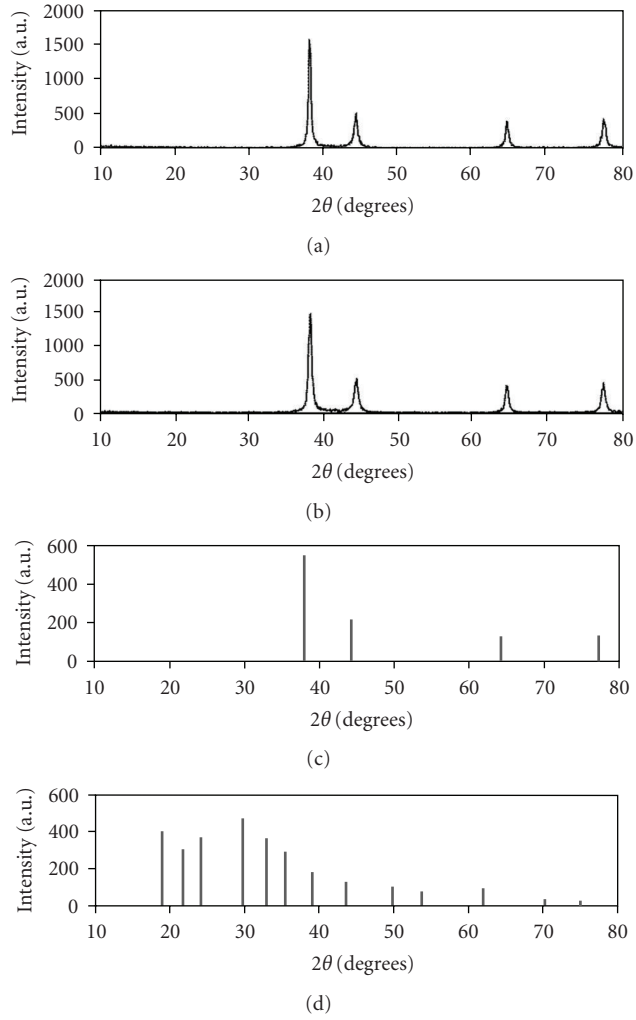

Figure 3: X-ray diffraction patterns for samples obtained in runs LC1 (a) and LC2 (b) from precipitation at 70°C in bicontinuous microemulsions containing 30 wt.% 0.5 M aqueous solution of $AgNO_3$ and 35 wt.% surfactant mixture. Standard patterns of silver (c) and $AgNO_3$ (d) are included.

composed of silver nanoparticles with diameters larger than 10 nm mixed with some isolated silver nanoparticles were found. It was not possible to identify any effect of dosing time. In contrast, the inspection of all micrographs obtained of samples from runs LC1 and LC2 reveals a mixture of isolated silver nanoparticles with diameters smaller than 10 nm and the worm-like nanostructures (Figure 5). Histograms obtained measuring over 200 isolated nanoparticles for run LC1 and over 400 for run LC2 are also included in Figure 5. Particle size data in histograms allowed to calculate values of 3.4 nm in average diameter and $\sigma = 0.8$ nm for run LC1. For run LC2, 3.3 and 0.8 nm for average diameter and σ, respectively, were obtained. From here, it appears that, at least in the studied interval, dosing time does not affect average particle size and particle size distribution of isolated silver nanoparticles.

Information on particle size can also be obtained by using data from X-ray diffraction patterns of samples from runs

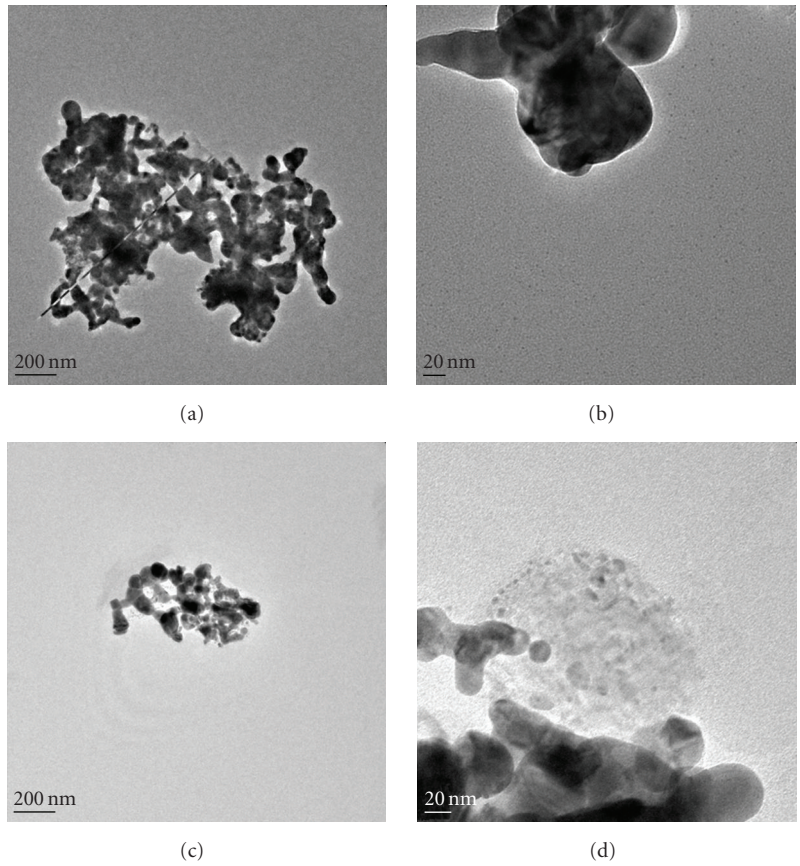

Figure 4: TEM micrographs for samples obtained in runs HC1 (a), HC2 (b), MC1 (c), and MC2 (d) from precipitation at 70°C in bicontinuous microemulsions containing 30 wt.% 0.5 M aqueous solution of $AgNO_3$ and 35 wt.% surfactant mixture.

LC1 and LC2 and the well-known Scherrer equation, which is represented as

$$d = \frac{K\lambda}{\beta \cos\theta}, \quad (1)$$

where d is the mean diameter of particle in nm; K is the dimensional factor (0.9); λ is the X-ray wavelength (0.154 nm); β is the line broadening at half the maximum intensity in radians; θ is the Bragg's angle. From these calculations, d values of 21 and 13.5 nm, for the particles from runs LC1 and LC2, respectively, were obtained. Differences between particle sizes determined by X-ray and TEM are large. This arises from the fact that estimation of mean particle size by X-ray takes into account all particles, that is, the isolated ones and those forming worm-like nanostructures. On one hand, in the particle size determination by TEM, only isolated nanoparticles were considered. From here, it is evident that in spite of formation of very small isolated silver nanoparticles, formation of worm-like nanostructures constituted of larger nanoparticles is important still at the lowest concentration of precipitating agent. Furthermore, it is worthy to note that the X-ray results indicate that the average diameter for particles from run LC1 was larger than that of run LC2 (21 versus 13.5 nm), while, according to TEM, the isolated particles in the samples from both runs are the same average size. This could be interpreted as that the worm-like nanostructures from LC2 run are constituted of smaller nanoparticles than those composing nanostructures from LC1 run and/or that the proportion of isolated nanoparticles in the sample from LC2 run is smaller than that in the sample from LC1 run. In any case, an inverse effect of dosing time of precipitating agent on average particle size might exist.

Table 2 shows the amount and purity of the products obtained in all reactions. Experimental yields and experimental yield/theoretical yield ratios are also included. Experimental yield was calculated as the grams of silver obtained per 100 g of total reaction mixture. Theoretical yield was the expected yield when all the silver in the $AgNO_3$ in the formulation was converted to metallic silver. Data in Table 2 indicates that by using bicontinuous microemulsions as a template it is possible to obtain silver nanostructures with experimental yields around 1.3. This value is higher than the highest theoretical yield (0.4) calculated from reported data in the literature on precipitation of silver nanoparticles in reverse microemulsions [10]. In addition, precipitation in bicontinuous microemulsions allows to reach higher reaction conversions (>80%) as deduced from the experimental yield/theoretical yield ratios.

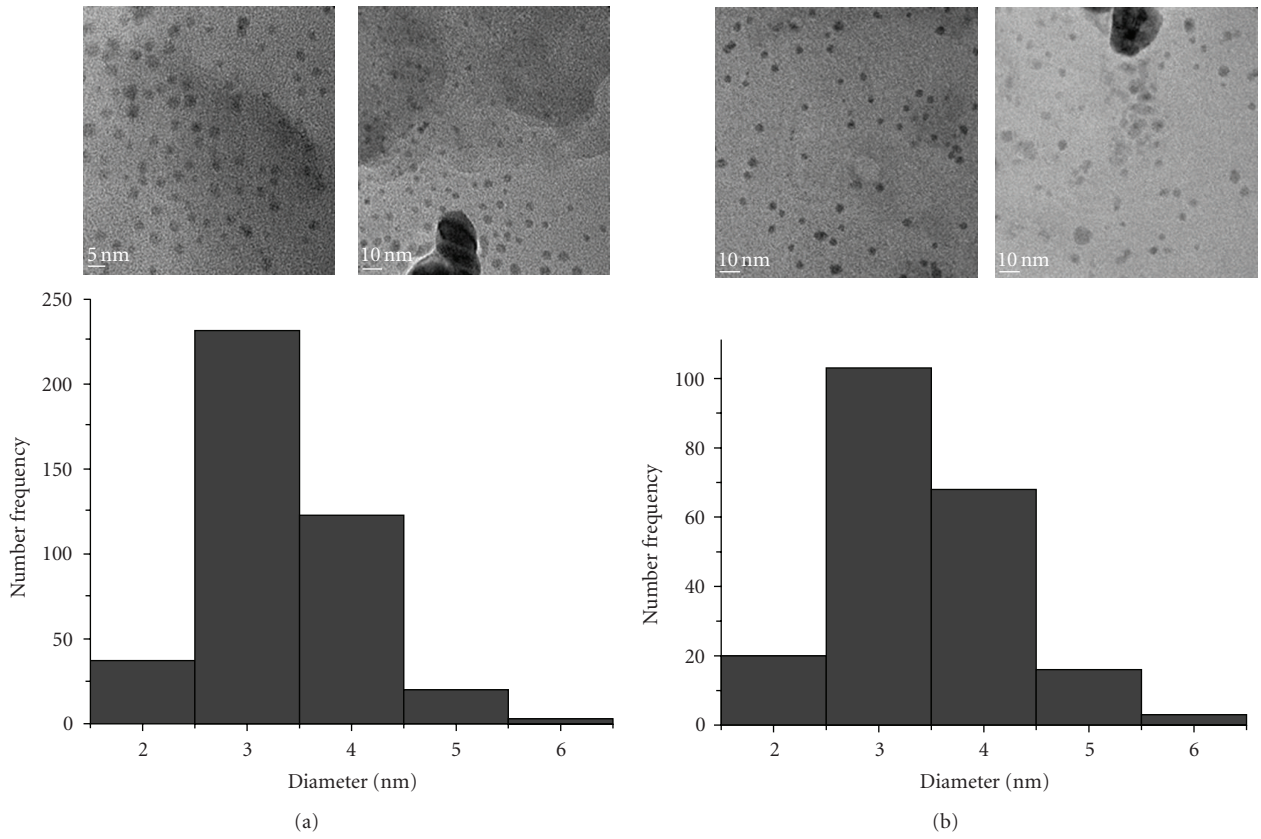

Figure 5: TEM micrographs and their histograms for particles obtained in LC1 (a) and LC2 (b) from precipitation at 70°C in a bicontinuous microemulsion containing 30 wt.% 0.5 M aqueous solution of $AgNO_3$ and 35 wt.% surfactant mixture.

Table 2: Characteristics and yields of products from precipitation reactions in bicontinuous microemulsions.

Run	Final product (g)	Purity (% silver)	Yield[a]	Yield ratio[b]
LC1	1.4888	97.7	1.26	0.88
LC2	1.6127	84.0	1.18	0.84
MC1	1.2732	98.4	1.14	0.82
MC2	1.3913	94.5	1.20	0.83
HC1	1.6862	84.6	1.34	0.86
HC2	1.5518	90.4	1.32	0.86

[a]g of silver/100 g of total mixture.
[b]experimental yield/theoretical yield.

In spite of the higher yields reached by precipitation of silver nanoparticles in bicontinuous microemulsions, only in the reactions carried out by dosing aqueous solutions with low $NaBH_4$ concentrations (LC1 and LC2), isolated nanoparticles with diameters smaller than 10 nm were synthesized. Precipitations carried out using higher $NaBH_4$ concentrations (runs HC1, HC2, MC1, and MC2) produce long worm-like nanostructures composed mainly of silver nanoparticles with diameters larger than 10 nm, regardless of dosing time of precipitating agent. Based on the location of $AgNO_3$ within bicontinuous nanostructures and how that comes into contact with the precipitating agent, a possible explanation for these results is provided as follows. When the precipitating agent is dosed on the microemulsion, the aqueous solution containing Na^+ and $^-BH_4$ ions diffuses into the channels in which Ag^+ and $^-NO_3$ ions are contained. Under these conditions, reduction reaction occurs for forming silver atoms. A fraction of these atoms clusters forming nuclei in some points of the channels. Thereafter, nuclei can grow by two mechanisms: (i) recruiting silver atoms (or clusters of silver atoms), which were formed as a result of the reduction reactions, and (ii) by aggregation as a consequence of interparticle collisions. In reverse microemulsions particles are protected by a surfactant film and so, usually only a small fraction of the interparticle collisions leads to aggregation [31]. Nevertheless, particles within the channels of bicontinuous microemulsions are not protected with any surfactant film. Thus, a greater particle aggregation should be expected in precipitation in bicontinuous microemulsion. On this basis, it is believed that when precipitations are carried out, dosing aqueous solutions with high $NaBH_4$ contents, zones inside microemulsions channels near to the contact point between the falling drop and the reaction mixture would contain high concentrations of precipitating agent. In these zones, precipitation reactions would occur very fast, leading to high particle concentrations. This way, interparticle collisions would be highly favored, and as a consequence, one-dimensional aggregation, which arise from the microemulsion channels acting as templates, would

occur, forming worm-like nanostructures. In contrast, when lower $NaBH_4$ concentrations are used, zones inside microemulsions channels near to the contact point between the falling drop and the reaction mixture will contain low concentrations of precipitating agent, leading to lower particle concentrations. So, interparticle collisions and as a consequence particle aggregation will be less favored, resulting in fewer worm-like nanostructures and a greater proportion of isolated small nanoparticles. The apparent inverse effect of dosing time on average particle size at low $NaBH_4$ concentrations suggested by X-ray results might be because a slow dosage would also lead to low particle concentrations within the microemulsions channels near to the contact point between the falling drop and the reaction mixture.

4. Conclusions

Precipitation in bicontinuous microemulsions when an aqueous solution of the precipitating agent ($NaBH_4$) at low concentration is dosed allows to obtain a mixture of isolated silver nanoparticles of average diameters around 3 nm and relatively narrow particle size distribution with worm-like nanostructures composed of silver nanoparticles with diameters larger than 10 nm. An inverse effect of dosing time of precipitating agent on average particle size might exist. Nevertheless, when precipitations are carried out at higher concentrations of $NaBH_4$, worm-like nanostructures are mainly obtained while isolated silver nanoparticles were very scarce. This was attributed to the development of local zones within the microemulsions channels with high particle concentrations, which favors interparticle collisions and one-dimensional aggregation. At higher and medium precipitating agent concentrations, no effect of dosing time on nanostructure type and particle size was identified, probably because of the very small studied interval. Moreover, experimental yields obtained in all runs were much higher than theoretical yields calculated from reported data in literature on precipitation of silver nanoparticles in reverse microemulsions. These findings may be used as basis for the further development of a method for preparing isolated silver nanoparticles of average diameters smaller than 10 nm, narrow particle size distributions, and yields higher than those typical in precipitation in reverse microemulsions. In fact, it is proposed that lower $NaBH_4$ concentrations than that used in the runs LC1 and LC2 would allow to synthesize exclusively isolated silver nanoparticles with diameters smaller than 10 nm and narrow particle size distributions. This issue, along with the increase in the dosing time of the precipitating agent, is explored at the present time by our research group.

Acknowledgments

CONACyT supported this research through grant CB-2007-84009. The authors, are grateful to Patricia Siller, Daniel Alvarado and Blanca Huerta for their technical assistance.

References

[1] L. S. Nair and C. T. Laurencin, "Silver nanoparticles: synthesis and therapeutic applications," *Journal of Biomedical Nanotechnology*, vol. 3, no. 4, pp. 301–316, 2007.

[2] H. Jiang, S. Manolache, A. C. L. Wong, and F. S. Denes, "Plasma-enhanced deposition of silver nanoparticles onto polymer and metal surfaces for the generation of antimicrobial characteristics," *Journal of Applied Polymer Science*, vol. 93, no. 3, pp. 1411–1422, 2004.

[3] A. Tripathi, N. Chandrasekaran, A. M. Raichur, and A. Mukherjee, "Antibacterial applications of silver nanoparticles synthesized by aqueous extract of *Azadirachta Indica* (Neem) leaves," *Journal of Biomedical Nanotechnology*, vol. 5, no. 1, pp. 93–98, 2009.

[4] J. L. Elechiguerra, J. L. Burt, J. R. Morones, et al., "Interaction of silver nanoparticles with HIV-1," *Journal of Nanobiotechnology*, vol. 3, no. 6, 2005.

[5] http://www.nanomet.ru/en/appl3.php.

[6] L. Esteban-Tejeda, F. Malpartida, A. Esteban-Cubillo, C. Pecharromán, and J. S. Moya, "The antibacterial and antifungal activity of a soda-lime glass containing silver nanoparticles," *Nanotechnology*, vol. 20, no. 8, Article ID 085103, 6 pages, 2009.

[7] M. Andersson, J. S. Pedersen, and A. E. C. Palmqvist, "Silver nanoparticle formation in microemulsions acting both as template and reducing agent," *Langmuir*, vol. 21, no. 24, pp. 11387–11396, 2005.

[8] P. Barnickel and A. Wokaun, "Synthesis of metal colloids in inverse microemulsions," *Molecular Physics*, vol. 69, no. 1, pp. 80–90, 1990.

[9] C. Petit, P. Lixon, and M.-P. Pileni, "In situ synthesis of silver nanocluster in AOT reverse micelles," *Journal of Physical Chemistry*, vol. 97, no. 49, pp. 12974–12983, 1993.

[10] L. A. Pavlyukhina, T. O. Zaikova, G. V. Odegova, S. A. Savintseva, and V. V. Boldyrev, "Silver clusters and nanoparticles: preparation in water-in-oil microemulsions and some physical properties," *Inorganic Materials*, vol. 34, no. 2, pp. 109–113, 1998.

[11] R. P. Bagwe and K. C. Khilar, "Effects of intermicellar exchange rate on the formation of silver nanoparticles in reverse microemulsions of AOT," *Langmuir*, vol. 16, no. 3, pp. 905–910, 2000.

[12] Z. Zhang, R. C. Patel, R. Kothari, C. P. Johnson, S. E. Friberg, and P. A. Aikens, "Stable silver clusters and nanoparticles prepared in polyacrylate and inverse micellar solutions," *Journal of Physical Chemistry B*, vol. 104, no. 6, pp. 1176–1182, 2000.

[13] W. Zhang, X. Qiao, J. Chen, and H. Wang, "Preparation of silver nanoparticles in water-in-oil AOT reverse micelles," *Journal of Colloid and Interface Science*, vol. 302, no. 1, pp. 370–373, 2006.

[14] W. Zhang, X. Qiao, and J. Chen, "Synthesis and characterization of silver nanoparticles in AOT microemulsion system," *Chemical Physics*, vol. 330, no. 3, pp. 495–500, 2006.

[15] W. Zhang, X. Qiao, and J. Chen, "Synthesis of nanosilver colloidal particles in water/oil microemulsion," *Colloids and Surfaces A*, vol. 299, no. 1–3, pp. 22–28, 2007.

[16] W. Zhang, X. Qiao, and J. Chen, "Formation of silver nanoparticles in SDS inverse microemulsions," *Materials Chemistry and Physics*, vol. 109, no. 2-3, pp. 411–416, 2008.

[17] S. Ezrahi, A. Aserin, and N. Garti, in *Handbook of Microemulsion Science and Technology*, P. Kumar and K. L. Mittal, Eds., chapter 7, p. 231, Marcel Dekker, New York, NY, USA, 1999.

[18] J. Esquivel, I. A. Facundo, M. E. Treviño, and R. G. López, "A novel method to prepare magnetic nanoparticles: precipitation in bicontinuous microemulsions," *Journal of Materials Science*, vol. 42, no. 21, pp. 9015–9020, 2007.

[19] A. L. Loo, M. G. Pineda, H. Saade, M. E. Treviño, and R. G. López, "Synthesis of magnetic nanoparticles in bicontinuous microemulsions. Effect of surfactant concentration," *Journal of Materials Science*, vol. 43, no. 10, pp. 3649–3654, 2008.

[20] Y. D. Sosa, M. Rabelero, M. E. Treviño, H. Saade, and R. G. López, "High yield synthesis of silver nanoparticles by precipitation in a high-aqueous phase content reverse microemulsions," *Journal of Nanomaterials*, vol. 2010, no. 10, Article ID 392572, 6 pages, 2010.

[21] H.-F. Eicke, M. Borkovec, and B. D. Das-Gupta, "Conductivity of water-in-oil microemulsions: a quantitative charge fluctuation model," *Journal of Physical Chemistry*, vol. 93, no. 1, pp. 314–317, 1989.

[22] M. Borkovec, H.-F. Eicke, H. Hammerich, and B. Das Gupta, "Two percolation process in microemulsions," *Journal of Physical Chemistry*, vol. 92, no. 1, pp. 206–211, 1988.

[23] J. F. Billman and E. W. Kaler, "Structure and phase behavior in five-component microemulsions," *Langmuir*, vol. 6, no. 3, pp. 611–620, 1990.

[24] A. Maitra, C. Mathew, and M. Varshney, "Closed and open structure aggregates in microemulsions and mechanism of percolative conduction," *Journal of Physical Chemistry*, vol. 94, no. 13, pp. 5290–5292, 1990.

[25] A. V. Sineva, D. S. Ermolat'ev, and A. V. Pertsov, "Structural transformations in a water-n-octane + chloroform-sodium dodecyl sulfate-*n* microemulsion," *Colloid Journal*, vol. 69, no. 1, pp. 89–94, 2007.

[26] L. M. Gan, T. H. Chieng, C. H. Chew, and S. C. Ng, "Microporous polymeric materials from microemulsion polymerization," *Langmuir*, vol. 10, no. 11, pp. 4022–4026, 1994.

[27] T. H. Chieng, L. M. Gan, C. H. Chew, et al., "Microporous polymeric materials by microemulsion polymerization: effect of surfactant concentration," *Langmuir*, vol. 11, no. 9, pp. 3321–3326, 1995.

[28] C. H. Chew, L. M. Gan, L. H. Ong, et al., "Bicontinuous structures of polymerized microemulsions: ^{1}H NMR self-diffusion and conductivity studies," *Langmuir*, vol. 13, no. 11, pp. 2917–2921, 1997.

[29] J. Liu, L. M. Gan, C. H. Chew, W. K. Teo, and L. H. Gan, "Nanostructured polymeric materials from microemulsion polymerization using poly(ethylene oxide) macromonomer," *Langmuir*, vol. 13, no. 24, pp. 6421–6426, 1997.

[30] C. H. Chew, T. D. Li, L. H. Gan, C. H. Quek, and L. M. Gan, "Bicontinuous-nanostructured polymeric materials from microemulsion polymerization," *Langmuir*, vol. 14, no. 21, pp. 6068–6076, 1998.

[31] M. M. Husein and N. N. Nassar, "Nanoparticle preparation using the single microemulsions scheme," *Current Nanoscience*, vol. 4, no. 4, pp. 370–380, 2008.